Absorption coefficient of phytoplankton: regional variations in the North Atlantic

V. A. Lutz[1,*], S. Sathyendranath[1,2], E. J. H. Head[2]

[1]Department of Oceanography, Dalhousie University, Halifax, Nova Scotia, Canada B3H 4J1
[2]Biological Oceanography Division, Bedford Institute of Oceanography, Box 1006, Dartmouth, Nova Scotia, Canada B2Y 4A2

ABSTRACT: The effect of major pigments on the absorption characteristics of phytoplankton were evaluated by comparing the *in vivo* absorption spectra of phytoplankton with pigment data obtained using high-performance liquid chromatography (HPLC) for samples of phytoplankton collected in the northwestern Atlantic Ocean, during spring. Four groups of spectra having distinct absorption characteristics and well-defined regional distributions were identified. The result of using general parameters to estimate the absorption coefficient of phytoplankton from any region, the 'general approach', was compared with the result of using specific parameters for each region, or the 'regional approach' Two methods of estimating the absorption coefficient were tested for each approach. These were: a 'single-pigment' method (Prieur & Sathyendranath 1981, Limnol Oceanogr 26:671–689). and a 'multi-pigment' method (Hoepffner & Sathyendranath 1991, Mar Ecol Prog Ser 73:11–23). It was shown that the regional approach performed better (<10% average error) than the general approach (<20% average error). Nevertheless, the results given by the general approach could be acceptable for some applications. The multi-pigment and the single-pigment methods performed equally well in the context of the regional approach, whereas in the general approach, the single-pigment method gave better results than the multi-pigment method. Overall, it appears that partitioning the oceans into regions according to their absorption characteristics should improve regional models of light transmission and the algorithms for detection of pigments by remote sensing.

KEY WORDS: Phytoplankton absorption · Phytoplankton pigments · Bio-optical models · North Atlantic · Regional variability

INTRODUCTION

Estimation of global oceanic primary production is an important goal in biological oceanography today, and it is recognized that models of primary production based on the use of phytoplankton biomass retrieved by remote sensing can be useful in addressing this problem (Smith et al. 1982, Platt & Herman 1983, Eppley et al. 1985, Platt 1986, Platt & Sathyendranath 1988, Platt et al. 1990, Morel 1991). In computations of primary production based on remotely sensed data, phytoplankton absorption plays an important role: first of all, it is a component of ocean-colour models used in algorithms for biomass retrieval (Gordon & Morel 1983, Sathyendranath & Morel 1983, Sathyendranath & Platt

1989a), secondly, it modifies light transmission underwater (Morel 1978, 1988, Sathyendranath & Platt 1988, Sathyendranath & Platt 1989b), and finally, it can modify the photosynthetic response of phytoplankton to available light through its effect on photosynthetic efficiency at low light (Smith et al. 1982, Kiefer & Mitchell 1983, Bidigare et al. 1987, Platt et al. 1988). Furthermore, knowledge of the absorption coefficient of phytoplankton is essential in studies of the biological contribution to the photon budget (Platt et al. 1984, Smith et al. 1989), thermal structure (Lewis et al. 1983, Lewis 1987) and mixed-layer dynamics (Sathyendranath et al. 1991).

A commonly used set of parameters in the estimation of primary production in the ocean comprises: the photosynthetic efficiency at low light normalised to biomass, α^B [mg C (mg chl a)$^{-1}$ h^{-1} (W m^{-2})$^{-1}$] (see Appendix 1 for list of symbols and definitions); the maximum

---

*E-mail: vlutz@is.dal.ca

production at high light normalised to biomass, P_m^B [mg C (mg chl a)$^{-1}$ h^{-1}]; and the diffuse attenuation coefficient of downwelling light, $K_d(\lambda)$ (m^{-1}), at each wavelength (λ) Spatial and temporal variations have been observed in the values of α^B and P_m^B (Platt & Sathyendranath 1988, Platt et al. 1992). To account for the variations in these parameters, Platt & Sathyendranath (1988) have proposed partitioning the ocean into biogeochemical provinces, within which the physiological parameters may be assumed to be quasi-stable for each season. In addition, however, it would be useful to have a similar classification for large-scale variations in phytoplankton-dependent optical properties such as phytoplankton absorption normalised to biomass, or biomass-specific $K_d(\lambda)$.

The shape of the absorption spectrum of a phytoplankton population is determined mainly by its pigment composition and by the flattening effect of particles in suspension (Duysens 1956, Kirk 1983, Sathyendranath et al. 1987). Changes in species composition and in physiological conditions affect the absorption properties of phytoplankton, and consequently $K_d(\lambda)$, since the latter depends on the absorption coefficient of phytoplankton, $a_{ph}(\lambda)$ (m^{-1}) (Kirk 1983, Smith et al. 1989). In models of light transmission in the open oceans, however, $a_{ph}(\lambda)$ and $K_d(\lambda)$ are often calculated as simple functions of chl a concentration (Morel 1978, Smith & Baker 1978, Sathyendranath & Platt 1988, Platt et al. 1994), and do not explicitly account for changes in phytoplankton population.

Several new methods have been proposed to estimate the absorption coefficient of phytoplankton based on the concentrations of all major pigments instead of just chl a (Bidigare et al. 1987, Bidigare et al. 1989, Bidigare et al. 1990, Hoepffner & Sathyendranath 1991). These 'multi-pigment' methods account for variations in pigment composition, although they do not necessarily account for the flattening effect. Implementation of multi-pigment methods requires knowledge of the concentrations of all of the major accessory pigments in addition to that of chl a.

In view of the essential role of $a_{ph}(\lambda)$ for the estimation of light penetration and primary production in the ocean, it is important to separate any systematic trends in $a_{ph}(\lambda)$ from random variations, and to determine if they are associated with changes in geographical location and/or season. It is also important to examine the relative merits of the different methods of estimating $a_{ph}(\lambda)$. With these objectives, the absorption characteristics and pigment composition of phytoplankton were studied during a spring cruise in the northwestern Atlantic.

The study covered an extensive area, which provided an opportunity for evaluating the variability in the absorption characteristics of phytoplankton over large spatial scales. We present here the results of an attempt to identify regions with similar absorption characteristics. Two different approaches to estimate the absorption coefficient of phytoplankton are compared: a 'general approach' in which it is assumed that the relationship between the absorption spectra of phytoplankton and the pigment concentrations does not vary significantly with geographical location; and a 'regional approach' which recognises systematic differences in the absorption characteristics of phytoplankton from different regions. In the regional approach, the absorption spectra are calculated using parameters specific for each region, whereas in the general approach a single set of general parameters is used to estimate the shape and magnitude of the absorption spectra of all the samples. Two methods of estimating the absorption coefficient are tested for each approach: (1) a 'single-pigment' method based on the use of a fixed shape of the spectrum which is scaled according to the concentration of chl a (Prieur & Sathyendranath 1981); and (2) a 'multi-pigment' method based on the use of the relationship between the concentrations of major pigments (chlorophylls a, b, c and carotenoids) and absorption at different wavelengths (Hoepffner & Sathyendranath 1991).

MATERIALS AND METHODS

Sampling. Samples were collected aboard the CSS 'Hudson', during a WOCE (World Ocean Circulation Experiment) cruise in April–May 1991, in the northwestern Atlantic. Samples for the determination of phytoplankton pigments and in vivo absorption were taken at standard oceanographic depths (1, 10, 20, 30, 40, 50, 75, and 100 m) from 8 l Niskin bottles attached to a rosette sampler. Seawater (0.25 to 1.0 l) was filtered onto GF/F (2.5 cm diameter) filters and stored in liquid nitrogen for later analysis of pigment content. For the in vivo absorption measurement, samples of 1 l of seawater were filtered through GF/F filters and frozen at –20°C.

Pigment analysis. Pigments were analysed following the method described by Head & Horne (1993). The HPLC (high-performance liquid chromatography) method was not able to separate zeaxanthin from lutein, i.e. they have the same retention time. But there is evidence suggesting that zeaxanthin dominates over lutein in the ocean (Everitt et al. 1990). Therefore, we assumed that all the absorption at that particular retention time was due to zeaxanthin; however, these values should be interpreted with caution. Divinyl-chl a and divinyl-chl b were identified by the presence of the corresponding divinyl-phaeophytins, after acidifying and running the samples a second time. It has been

observed that substantial degradation of phytoplankton pigments can occur in certain species of diatoms (with high chlorophyllase activity) within a few minutes after filtration (Stramski 1990). However, HPLC analysis showed very low concentrations of chlorophyllide a (ratio chlorophyllide a:chl a <0.2, with only 14 among 279 samples having a ratio >0.1), which is a degradation product produced by the action of the chlorophyllase enzyme.

In vivo absorption. The in vivo absorption spectra of total particulate matter were measured on GF/F glass-fiber filters (Yentsch 1962, Kiefer & SooHoo 1982, Mitchell & Kiefer 1984, Kishino et al. 1985) using a Beckman DU-64 spectrophotometer. Frozen filters were allowed to thaw prior to the measurements. In our study, samples for absorption measurement and for pigment analysis were handled in the same way with the only difference being that samples for HPLC were stored at –70°C and samples for absorption were stored at –20°C. To investigate the possibility of pigment degradation in the samples stored at –20°C, the pigment composition of replicates (one stored at –20°C and the other at –70°C) of a sample from a station where diatoms were predominant (Stn 6) were compared. This comparison showed <8% difference in the concentration of all the pigments present in the sample. Therefore, even though we cannot be sure that there was no pigment degradation in the samples preserved at –20°C, there is no evidence that major degradation had occurred.

The filters were placed in a special sample holder close to the photomultiplier to avoid loss of forward-scattered light (Mitchell & Kiefer 1984). The filters were wetted with filtered seawater before reading, and a new filter, also wetted with seawater, was used as a blank. The optical density or absorbance (D) was recorded between 350 and 750 nm. The value measured at 750 nm was subtracted from the rest of the spectrum, assuming that this optical density was due to non-pigmented substances and that its effect was spectrally neutral (Sathyendranath et al. 1987, Bricaud & Stramski 1990).

The absorption coefficient of particles on the filter, $a_{pf}(\lambda)$ (m^{-1}), was obtained as:

$$a_{pf}(\lambda) = 2.3\, D(\lambda)/X \tag{1}$$

where X is the height in meters of the water column filtered, given by V/S, where V is volume of seawater filtered (m^3) and S is filtering area of the filter (m^2); and 2.3 is the conversion factor for transforming decimal logarithms to natural logarithms.

The values of absorption coefficient (m^{-1}) measured on filters were corrected for the pathlength amplification factor, β (Butler 1962, Kiefer & SooHoo 1982), which is defined as the ratio of the optical thickness of a dif-

fusing material to its geometric thickness; i.e. β represents the amplification of the path of light through the glass fiber filter due to multiple scattering. To correct for the pathlength amplification the following quadratic equation proposed by Hoepffner & Sathyendranath (1992) based on uni-algal cultures was used:

$$a_p(\lambda) = 0.31[a_{pf}(\lambda)] + 0.57[a_{pf}(\lambda)]^2 \tag{2}$$

where $a_p(\lambda)$ is the absorption coefficient of particles in suspension. This is very similar to the equation more recently proposed by Cleveland & Weidemann (1993) which was also derived from culture work and for which they reported characteristic errors <2% in the value of $a_p(\lambda)$, and a maximum of 20% for a single sample in the yellow wavelengths.

Corrections were made for detrital absorption using the theoretical approach proposed by Hoepffner & Sathyendranath (1993), which assumes an exponential shape for detrital absorption (Roesler et al. 1989, Bricaud & Stramski 1990). According to this method, the total absorption by particles can be defined as:

$$a_p(\lambda) = a_{ph}(440)\, a'_{ph}(\lambda) + a_d(440)\, \exp[-q(\lambda - 440)] \tag{3}$$

where the first term on the right-hand side represents absorption by phytoplankton, and the second term that by detritus. Here, the absorption from particles, $a_p(\lambda)$, is known from measurements; the absorption coefficient of phytoplankton normalised to 440 nm, $a'_{ph}(\lambda)$, was taken from Hoepffner & Sathyendranath (1993); and the values of absorption by phytoplankton and detritus at 440 nm, $a_{ph}(440)$ and $a_d(440)$ respectively, and the exponent q, were obtained by non-linear regression. Finally, the absorption coefficient of phytoplankton was obtained by subtracting the estimated absorption of detritus from the measured particle absorption according to:

$$a_{ph}(\lambda) = a_p(\lambda) - a_d(440)\, \exp[-q(\lambda - 440)] \tag{4}$$

The values of $a_{ph}(\lambda)$ estimated in this way are referred to as 'observed values of $a_{ph}(\lambda)$' in the rest of the text.

Hoepffner & Sathyendranath (1993) have shown that even small errors in the estimation of $a_{ph}(440)$ by non-linear regression may induce high errors (up to a factor of 3) in the estimation of $a_d(440)$, in cases where the absorption by detritus is several times less than the absorption by phytoplankton. However, the error in the detritus absorption values will not introduce a severe problem in the estimation of the absorption of phytoplankton, since typically, $a_d(\lambda)$ values are much smaller than $a_{ph}(\lambda)$ values.

The absorption spectra of phytoplankton were decomposed into Gaussian bands following the method of Hoepffner & Sathyendranath (1991). The Gaussian curves represent the absorption by the main pigments: chl a, chl b, chl c (the sum of chlorophylls $c_1 + c_2$ and

c_a), and carotenoids (i.e. the sum of the concentrations of all the carotenoids found in the sample). Each Gaussian band is defined by the wavelength of the band center, λ_i, the halfwidth of the band, W_i, and the peak height of the band, $p_i(\lambda_i)$. The curve-fitting program used was the same as that used by Hoepffner & Sathyendranath (1991). We also used the initial values of the centers and the halfwidths of the bands given by Hoepffner & Sathyendranath (1991) (see their Table 4). The initial guesses for the heights of the bands were adjusted according to the magnitude of the absorption spectra. Then, from the output, the average values of the band centers and halfwidths were computed for application in the 'general approach' and the 'regional approach' (see Table 4).

DATA ANALYSIS AND RESULTS

Identification of groups with similar absorption characteristics

The identification of groups of similar absorption characteristics was made according to the shape of the absorption spectra: First, the corrected phytoplankton absorption spectrum of each sample was normalised to 1 at 440 nm. Then, the samples were grouped according to the shape of their absorption spectra, based on a visual inspection, and the average spectrum of each group was computed. The mean spectra for each group were compared, and groups with similar mean spectra were then recombined into a single group, resulting in a final set of 4 groups with distinct absorption characteristics (Fig 1). In the stations showing a high degree of stratification, the absorption spectra from depths below the thermocline usually showed very low values of absorption (close to or below the limit of detection of the spectrophotometer), and therefore they were not considered in the analysis. This might have contributed to the fact that all the samples from a station fell into the same group. The geographical distribution of the groups is shown in Fig. 2. The difference among groups was tested at a set of selected wavelengths (412, 490, 555, and 670 nm; 443 was excluded because of the normalisation at 440 nm) that will be monitored by the ocean-colour satellite SeaWiFS, to be launched by NASA (Hooker et al. 1992). At these wavelengths the relative absorption values from the 4 groups were found to be significantly different (at $p \leq 0.0001$) using a 1-way analysis of variance.

The ratios of the predominant accessory pigments to chl a in each group are depicted in Fig 3. These pigment ratios were found to be significantly different between groups (at $p \leq 0.0001$) using a Kruskal-Wallis 1-way analysis of variance on ranks. The pigment composition was used to characterize the phytoplankton composition of the groups (Gieskes et al. 1988, and review by Wright et al. 1991). Notice that some of the pigments used as markers are not exclusive to one group of algae (Rowan 1989, Wright et al. 1991, Johnsen et al. 1994a) and since no identification of phytoplankton species by microscopy was made, all the references to algal groups in this study should be taken as the most probable but not as the definitive or the only possible composition of the phytoplankton assemblages. Divinyl-chl a and b were detected mainly in Group C (ratio divinyl-chl a:chl a ~0.1 to 0.7) and in minor concentrations at 2 stations (Stns 45 and 52) of Group B (ratio divinyl-chl a:chl a <0.15). In all the cases the values of chl a considered for the analysis represent the sum of normal chl a and divinyl-chl a; similarly, the chl b concentrations used represent the sum of normal chl b and divinyl-chl b. Since divinyl-chlorophylls were present almost exclusively in Group C, no special treatment was carried out to distinguish between normal and divinyl-chlorophylls during the calculation of specific peak heights, or absorption coefficients. Thus, the specific coefficients of chlorophylls for Group C represent the effect of the mixture of the 2 types: normal and divinyl-chlorophylls. It is also worth mentioning that, since the determination of phycobilins was not possible with the HPLC analysis used, absorption at any wavelength by these pigments, if present, would be attributed to other pigments absorb-
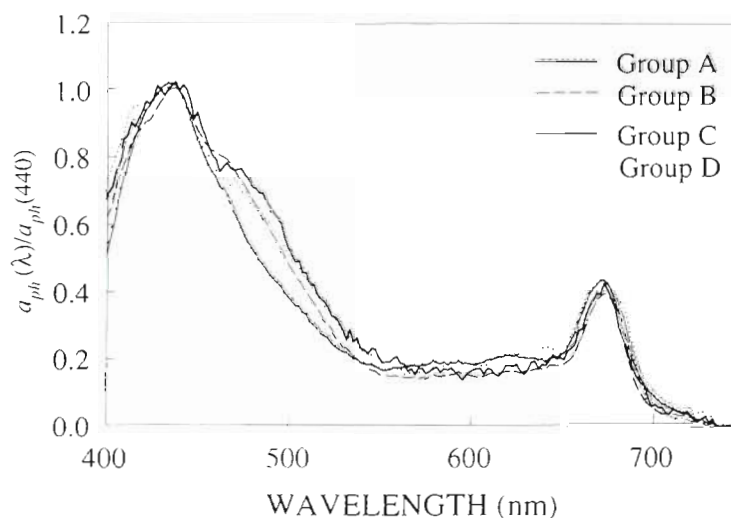

Fig. 1 Average phytoplankton absorption spectra [$a_{ph}(\lambda)$] of the 4 groups identified in this work. All the spectra are normalised to 1 at 440 nm

ing at the same wavelengths (~480 to 600 nm). Phycobilins are present in the phytoplanktonic groups cyanophytes and cryptophytes. The concentration of cryptophytes in these samples may be negligible since the concentrations of alloxanthin (a characteristic pigment of cryptophytes) was always low (ratio alloxanthin:chl *a* <0.13, being ~0.1 in only 4 out of 279 samples and <0.07 in the rest). On the other hand, the concentration of zeaxanthin (a pigment characteristic of cyanophytes) was high only in Group C (see Fig. 3), and this pigment can also be linked to the presence of prochlorophytes. Therefore, the effect of phycobilins, if any, was probably confined to Group C.

For each group, 25% of the samples, selected randomly, were kept aside to be used later for testing the methods. The remaining samples were used to calculate the parameters required to estimate the absorption coefficient of phytoplankton using the different methods.

Calculation of absorption parameters

Although a linear function could, to some extent, fit the relationship between absorption and pigment concentration (Lutz 1994), it was found that a non-linear function gave a better representation of that relationship. Several non-linear functions have been used in the past to describe the relationship between absorption coefficient at a given wavelength and the corresponding pigment concentration:

Prieur & Sathyendranath (1981), Yentsch & Phinney (1989), and Morel (1991) used a power function of the form:

$$a_{ph}(\lambda) = \delta C^\kappa \tag{5}$$

with δ and κ as the 2 fitted parameters, and C as the pigment concentration. Cleveland (1995) suggested the use of another equation:

$$a_{ph}(\lambda) = \phi C + \omega C^2 \tag{6}$$

where ϕ and ω are the 2 parameters of the second-order polynomial with zero intercept; and Sathyendranath & Platt (1988) proposed using the equation for a rectangular hyperbola (of the form commonly used to describe Michaelis-Menten type kinetics):

$$a_{ph}(\lambda) = \frac{\gamma C}{\epsilon + C} \tag{7}$$

which also required 2 parameters (γ and ϵ).

To choose among these, each one of these functions was fitted to one of our data sets (absorption at 440 nm and chl *a* from all the samples) (Fig. 4). All the functions fitted the data equally well; therefore, we use additional criteria in the selection process.
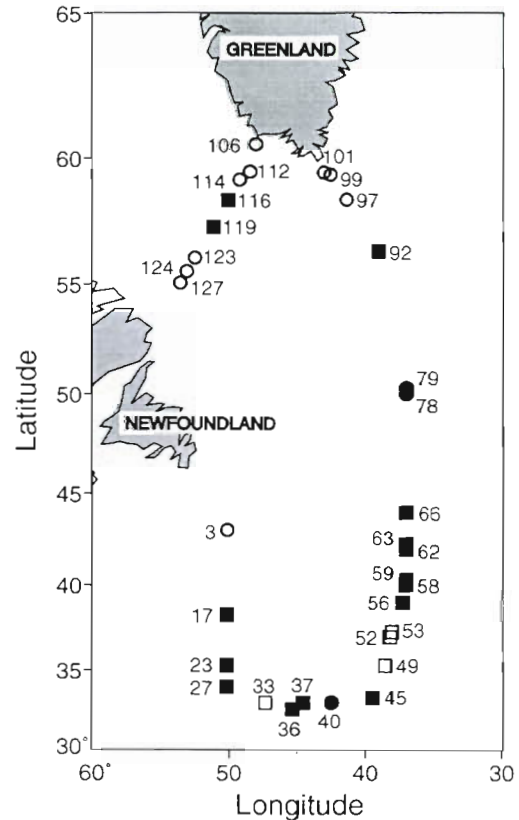

Fig. 2. Geographical distribution of the 4 groups (O) Group A; (■) Group B; (□) Group C; (●) Group D
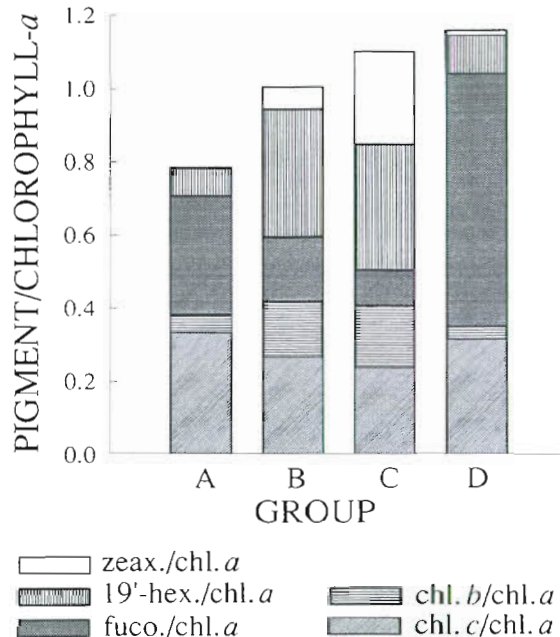

Fig. 3. Ratio of the main accessory pigments (chl *b*, chl *c*, fucoxanthin, 19'-hexanoyloxyfucoxanthin, and zeaxanthin) to chl *a* in the 4 groups (A, B, C, D). Here chl *c* is taken as the sum of chlorophylls $c_1 + c_2 + c_3$
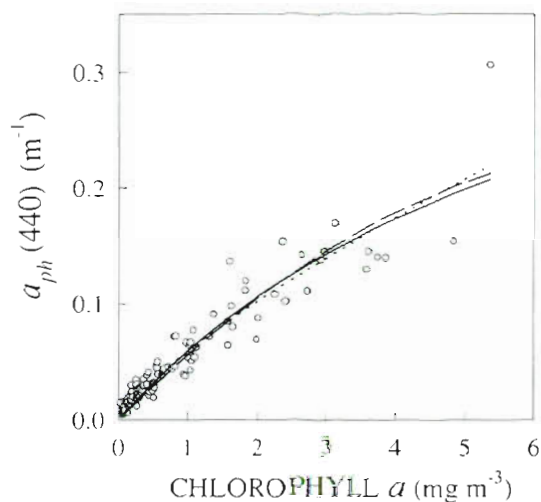
Fig. 4. Different functions fitted to describe the relationship between absorption at 440 nm and chl a concentrations. Dotted line: power function; solid line: rectangular hyperbola function; dashed line: second-order polynomial
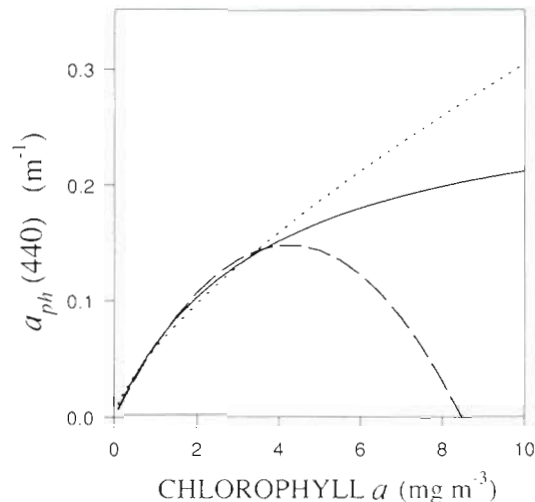

Fig. 5. The different functions for computing phytoplankton absorption [a_{ph}(440)] from pigment concentrations extended beyond the fitted range of chl a concentrations. Dotted line: power function; solid line: rectangular hyperbola function; dashed line: second-order polynomial

For all these functions, the slope of the curves approaches a maximum at the origin. The slope defines the rate of change of absorption per unit change in pigment, or, in other words, the specific absorption coefficient. Since the maximum value of the specific absorption coefficient is of general interest, we examined the slope near the origin for each of the functions. For example, we can rearrange Eq. (7) in such a way that the slope at the origin appears explicitly in the equation:

$$a_{ph}(\lambda) = \frac{a_m\, a^*_m C}{a_m + a^*_m C} \qquad (8)$$

where we have replaced γ/ϵ with a^*_m, the initial slope near the origin of the absorption versus pigment concentration curve (maximum specific absorption coefficient), and γ with a_m, the asymptotic maximum value of a_{ph}. Both the polynomial and the rectangular hyperbola functions have well-defined initial slopes. On the other hand, for the power function, this value approaches infinity at the origin, which is not a desirable quality. Therefore we abandoned the use of the power function. We next examined how the functions behaved when the results were extrapolated towards higher values. Fig 5 shows that none of the curves performs ideally: the slope of the rectangular hyperbola curve (a^*_{ph}) approaches zero (as absorption approaches ~0.28 m^{-1}) asymptotically, whereas the slope of the second-order polynomial decreases very rapidly and becomes negative above a threshold value of concentration. This effect is seen more clearly if we plot in a^*_{ph} normalised to a^*_m, as a function of C (Fig 6). This quantity changes rapidly for the second-

order polynomial, with the slope becoming negative at $C \approx 5$ mg m^{-3}, while for the rectangular hyperbola function the changes are more gradual, reaching zero asymptotically at $C > 20$ mg m^{-3}. Both of these curves are purely empirical, and they are meant to be applied only within the range of values for which they were established. Should a requirement for extrapolation arise, however, the rectangular hyperbola function would perform better than the polynomial function. Therefore the rectangular hyperbola function was used in this paper to describe the empirical relationship between absorption and pigment concentrations.
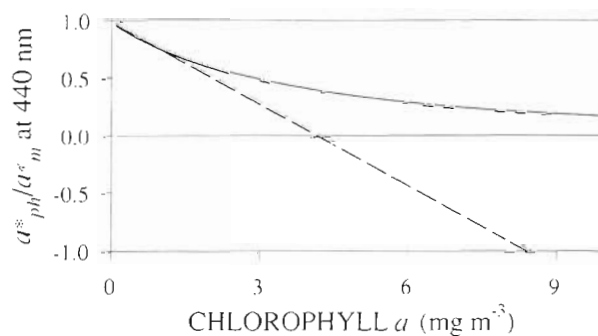

Fig. 6. Changes in the slope of the rectangular hyperbola and second-order polynomial functions relative to the slope at the origin; solid line: rectangular hyperbola function; dashed line: second-order polynomial. Since the slope represents the specific absorption coefficient, the plotted functions represent relative changes in specific absorption, with increase in chl a

'Single-pigment' method

The phytoplankton absorption at 440 nm was parameterised as a function of chl a concentration (C) using Eq. (8), with λ = 440 nm. These parameters were obtained by fitting Eq. (8) to a set of $a_{ph}(440)$ and C, using the Marquardt-Levenberg method (Sigmaplot for Windows 1.02, Jandel Scientific). This procedure was followed for the 'general approach' (Fig. 4, Table 1; all the data combined), and for the 'regional approach' (Fig. 7, Table 1; each group treated separately).

'Multi-pigment' method

The peak height $[p_i(\lambda_i)]$ at the wavelength of the center of the ith Gaussian band was parameterised as a function of its corresponding pigment concentration (C_i) as follows:

$$p_i(\lambda_i) = \frac{p_m(i)\, p^{\bullet}_m(i)\, C_i}{C_i\, p^{\bullet}_m(i) + p_m(i)} \quad (9)$$

where $p^{\bullet}_m(i)$ (maximum specific peak height) and $p_m(i)$ are the parameters that define the relationship between peak height and pigment concentration for the ith Gaussian curve. These parameters were also computed for the 'general approach' (Fig. 8, Table 2; all the samples combined), and for the 'regional approach' (Fig. 9, Table 3; each group treated separately). At some wavelengths the data set was not ex-

tensive enough to compute the value of maximum absorption $p_m(i)$ with reasonable accuracy, and therefore only $p^{\bullet}_m(i)$ could be determined.

Evaluation of the methods

The performance of the methods used in both the 'general' and the 'regional' approaches was tested by reconstructing the absorption spectra of the samples not used to establish the methods, and by comparing the results of the reconstructed spectra with the observations, as described below.

Table 1. Results for the 'general' and 'regional' approaches, 'single-pigment' method. Values of a_m (m^{-1}) and $a^{\bullet}_m$ [m^{-1} (mg chl a m^{-3})$^{-1}$] fitted to the rectangular hyperbola equation (Eq. 8) used to parameterise the absorption at 440 nm as a function of chl a concentration. The coefficient of determination (r^2) for the fits and the number of pairs of observations (N) are given

Group	a_m	SE	$a^{\bullet}_m$	SE	r^2	N
A	1.00	5.9×10^{-1}	0.06	5.8×10^{-3}	0.84	42
B	0.11	2.1×10^{-2}	0.11	1.1×10^{-2}	0.77	52
C	0.09	3.2×10^{-2}	0.11	1.7×10^{-2}	0.88	15
D	0.26	5.2×10^{-2}	0.07	1.5×10^{-2}	0.99	8
Pooled	0.48	7.3×10^{-2}	0.07	4.1×10^{-3}	0.89	117

Table 2. Results for the 'general approach', 'multi-pigment' method. Values of the parameters $p^{\bullet}_m(i)$ [m^{-1}(mg pigment m^{-3})$^{-1}$] and $p_m(i)$ (m^{-1}) for the rectangular hyperbola equation (Eq. 9) used to parameterise the peak heights using the pigment concentrations[a] which correspond to each Gaussian band. The coefficient of determination (r^2), and the number of pairs of observations (N) are also given

Gaussian band (i)	$p_m(i)$	SE	$p^{\bullet}_m(i)$	SE	r^2	N
1	0.37	1.1×10^{-1}	0.03	2.1×10^{-3}	0.85	117
2	0.15	1.8×10^{-2}	0.03	1.6×10^{-3}	0.90	117
3	0.43	7.4×10^{-2}	0.06	3.7×10^{-3}	0.88	117
4	0.40	1.9×10^{-2}	0.06	4.2×10^{-3}	0.84	117
5	0.04	1.5×10^{-2}	0.16	2.9×10^{-2}	0.47	113
6	0.11	1.2×10^{-2}	0.05	3.1×10^{-3}	0.80	117
7	0.07	9.9×10^{-3}	0.02	1.2×10^{-3}	0.80	117
8	0.07	1.1×10^{-2}	0.03	2.7×10^{-5}	0.85	117
9	0.08	1.8×10^{-2}	0.01	4.6×10^{-4}	0.89	117
10	0.05	6.4×10^{-3}	0.02	1.3×10^{-3}	0.90	117
11	0.01	4.1×10^{-3}	0.05	8.9×10^{-3}	0.48	113
12	0.27	5.4×10^{-2}	0.02	1.2×10^{-3}	0.92	117
13	0.03	9.6×10^{-3}	0.01	3.8×10^{-4}	0.73	117

[a]Ranges of pigment concentration for which the parameters are given:

chl a: 0–5.4 mg m^{-3}; chl c: 0–1.9 mg m^{-3}; chl b: 0–0.2 mg m^{-3}; carot.: 0–3.0 mg m^{-3}
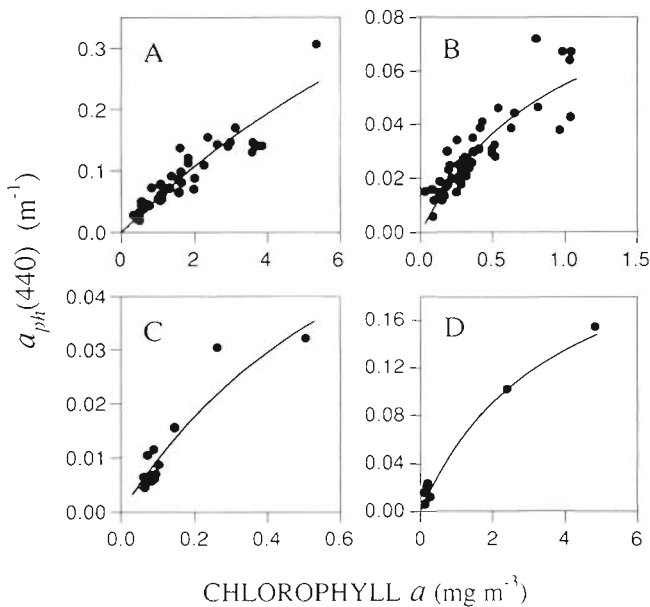
Fig. 7 Phytoplankton absorption at 440 nm $[a_{ph}(440)]$ as a function of chl a concentration and curves fitted to the data using the rectangular hyperbola equation. 'Regional approach', 'single-pigment' method, Groups A, B, C, and D
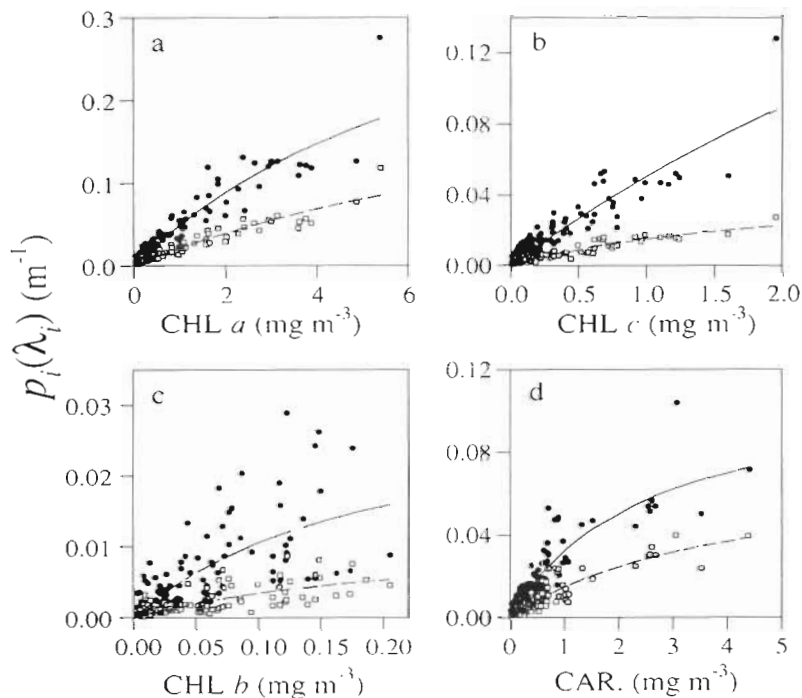
Fig. 8. Peak height $[p_i(\lambda_i)]$ as a function of the related pigment concentration and curves fitted to the data using the rectangular hyperbola equation. 'General approach', 'multi-pigment' method. (a) ($\bullet$, ———) chl a vs $p_3(\lambda_3)$; ($\square$, — · —) chl a vs $p_{12}(\lambda_{12})$. (b) ($\bullet$, ———) chl c vs $p_4(\lambda_4)$; ($\square$, — —) chl c vs $p_{10}(\lambda_{10})$. (c) ($\bullet$, ———) chl b vs $p_5(\lambda_5)$; ($\square$, — —) chl b vs $p_{11}(\lambda_{11})$. (d) ($\bullet$, ———) carotenoids vs $p_6(\lambda_6)$; ($\square$, — —) carotenoids vs $p_7(\lambda_7)$
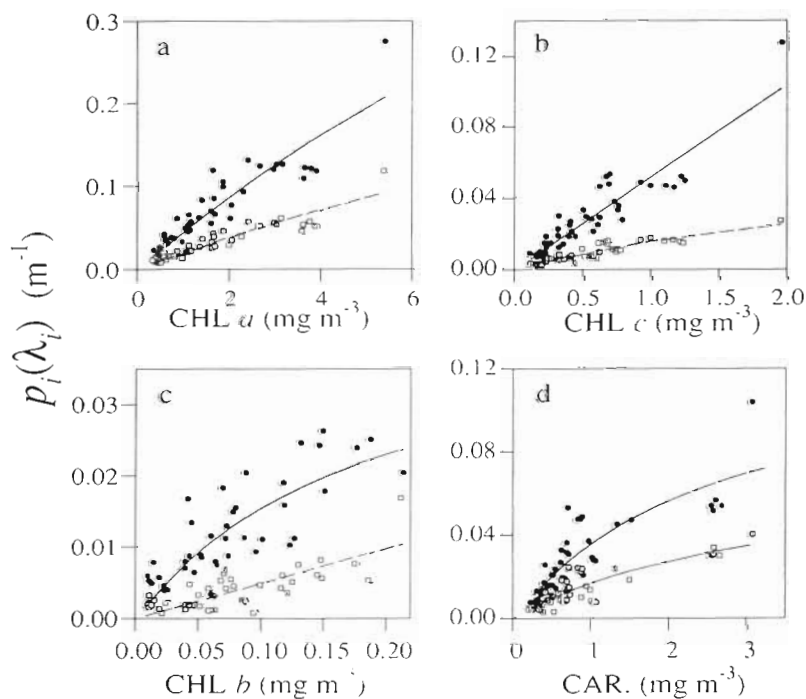
Fig. 9. Peak height $[p_i(\lambda_i)]$ as a function of pigment concentration and curves fitted to the data using the rectangular hyperbola equation. 'Regional approach', 'multi-pigment' method for Group A: (a) ($\bullet$, ———) chl a vs $p_3(\lambda_3)$; ($\square$, — —) chl a vs $p_{12}(\lambda_{12})$. (b) ($\bullet$, ———) chl c vs $p_4(\lambda_4)$; ($\square$, — —) chl c vs $p_{10}(\lambda_{10})$. (c) ($\bullet$, ———) chl b vs $p_5(\lambda_5)$; ($\square$, — —) chl b vs $p_{11}(\lambda_{11})$. (d) ($\bullet$, ———) carotenoids vs $p_6(\lambda_6)$; ($\square$, — —) carotenoids vs $p_7(\lambda_7)$

'Single-pigment' method

The absorption coefficients of each group ('regional approach'), or that of all the samples combined ('general approach'), were reconstructed by scaling the corresponding average spectrum normalised to 440 nm,

$a'_{ph}(\lambda)$ (Figs. 1 & 12) to the values of absorption at 440 nm, according to:

$$a_{ph}(\lambda) = a'_{ph}(\lambda)a_{ph}(440) \qquad (10)$$

where $a_{ph}(440)$ was calculated using the relationship between chl a concentrations and $a_{ph}(440)$ (Table 1).

'Multi-pigment' method

The reconstruction by the 'multi-pigment' method was carried out as described in Hoepffner & Sathyendranath (1991), by adding all the 13 Gaussian bands, according to:

$$a_{ph}(\lambda) = \sum_{i=1}^{13} p_i(\lambda_i)\exp\left[-\frac{(\lambda - \lambda_i)^2}{2W_i^2}\right] \qquad (11)$$

The values of the halfwidths, W_i (nm), and centers, λ_i (nm), of the bands were the calculated average values for the 'general approach' or the 'regional approach' (Table 4); the peak heights of each band, $p_i(\lambda_i)$ (m^{-1}), were estimated from the corresponding parameters $p_m(i)$ and $p^{\bullet}_m(i)$ (Tables 3 & 4).

Comparison with independent observations

To evaluate how well the different methods of reconstruction reproduce the shape of the absorption spectrum of phytoplankton, the relative errors in the reconstructed spectra (the difference between observed and calculated values scaled to the observed value) were computed. The spectrally resolved average relative errors and the standard errors of the averages are presented for each method used in the 2 approaches (Fig 10); errors from 700 nm towards the infrared are not considered since absorption by pigments is negligible at those wavelengths.

The correlation between the observed absorption coefficients and the calculated absorption coefficients

Table 3. Results for the 'regional approach', 'multi-pigment' method. Values of the parameters $p^{\bullet}_m(i)$ [m^{-1} (mg pigment m^{-3})$^{-1}$] and $p_m(i)$ (m^{-1}) for the rectangular hyperbola equation (Eq. 9) used to parameterise the peak heights using the pigment concentrations which correspond to each band. The coefficient of determination (r^2), and the number of pairs of observations (N), are also given

Gaussian band (i)	Group A						Group B					
	$p_m(i)$	SE	$p^{\bullet}_m(i)$	SE	r^2	N	$p_m(i)$	SE	$p^{\bullet}_m(i)$	SE	r^2	N
1	–	–	0.02	8.0×10^{-4}	0.85	42	0.06	9.6×10^{-3}	0.07	7.8×10^{-3}	0.74	52
2	0.22	6.7×10^{-2}	0.02	2.5×10^{-3}	0.84	42	0.04	7.4×10^{-3}	0.04	4.1×10^{-3}	0.77	52
3	1.04	6.8×10^{-1}	0.05	5.1×10^{-3}	0.83	42	0.10	1.7×10^{-2}	0.09	8.1×10^{-3}	0.79	52
4	–	–	0.05	2.1×10^{-3}	0.83	42	0.03	4.6×10^{-3}	0.16	1.8×10^{-2}	0.75	52
5	0.04	1.2×10^{-2}	0.24	4.3×10^{-2}	0.66	42	0.01	3.5×10^{-3}	0.12	2.4×10^{-2}	0.46	50
6	0.13	2.9×10^{-2}	0.05	6.4×10^{-2}	0.72	42	0.04	8.0×10^{-3}	0.05	5.7×10^{-3}	0.72	52
7	0.07	1.7×10^{-2}	0.02	2.6×10^{-3}	0.76	42	0.02	4.6×10^{-3}	0.02	2.1×10^{-3}	0.70	52
8	0.09	3.5×10^{-2}	0.03	4.2×10^{-3}	0.73	42	0.01	1.2×10^{-3}	0.08	1.1×10^{-2}	0.63	52
9	0.16	1.0×10^{-1}	0.01	6.7×10^{-4}	0.86	42	0.01	2.1×10^{-3}	0.01	1.2×10^{-2}	0.73	52
10	0.07	2.5×10^{-2}	0.02	1.7×10^{-3}	0.85	42	0.01	1.2×10^{-3}	0.05	6.7×10^{-3}	0.64	52
11	–	–	0.05	3.3×10^{-3}	0.58	42	0.01	1.3×10^{-3}	0.04	5.2×10^{-3}	0.64	50
12	0.46	2.9×10^{-1}	0.02	2.0×10^{-3}	0.85	42	0.04	8.1×10^{-3}	0.04	3.3×10^{-3}	0.81	52
13	0.05	3.3×10^{-2}	0.01	6.1×10^{-4}	0.63	42	0.01	4.4×10^{-4}	0.01	1.5×10^{-3}	0.35	52

Ranges of pigment concentration for which the parameters are given:

chl a: 0–5.4 mg m^{-3}; chl c: 0–1.9 mg m^{-3};   chl a: 0–1.0 mg m^{-3}; chl c: 0–0.3 mg m^{-3};
chl b: 0–0.2 mg m^{-3}; carot.: 0–3.0 mg m^{-3} chl b: 0–0.2 mg m^{-3}; carot.: 0–1.0 mg m^{-3}

Gaussian band (i)	Group C						Group D					
	$p_m(i)$	SE	$p^{\bullet}_m(i)$	SE	r^2	N	$p_m(i)$	SE	$p^{\bullet}_m(i)$	SE	r^2	N
1	–	–	0.05	3.9×10^{-3}	0.83	15	0.63	5.4×10^{-1}	0.03	5.7×10^{-3}	0.96	8
2	0.02	6.1×10^{-1}	0.05	7.0×10^{-3}	0.85	15	0.11	2.2×10^{-2}	0.03	4.9×10^{-3}	0.99	8
3	0.07	2.4×10^{-2}	0.09	1.1×10^{-2}	0.90	15	0.27	1.0×10^{-1}	0.05	1.2×10^{-2}	0.97	8
4	–	–	0.07	2.3×10^{-2}	0.70	15	0.29	4.8×10^{-1}	0.04	1.1×10^{-2}	0.96	8
5	0.01	1.1×10^{-3}	0.15	2.5×10^{-2}	0.88	15	–	–	0.21	4.2×10^{-2}	0.97	7
6	–	–	0.03	4.5×10^{-3}	0.61	15	0.13	6.6×10^{-2}	0.03	1.2×10^{-2}	0.97	8
7	0.01	3.1×10^{-3}	0.03	5.9×10^{-3}	0.58	15	0.09	7.0×10^{-2}	0.01	6.3×10^{-3}	0.95	8
8	0.01	1.2×10^{-3}	0.08	2.1×10^{-2}	0.62	15	0.03	7.2×10^{-3}	0.05	2.0×10^{-2}	0.97	8
9	0.01	5.6×10^{-4}	0.16	1.7×10^{-4}	0.87	15	0.03	7.0×10^{-3}	0.01	1.9×10^{-3}	0.98	8
10	0.01	1.5×10^{-3}	0.06	1.6×10^{-2}	0.61	15	0.02	4.3×10^{-3}	0.04	1.8×10^{-2}	0.97	8
11	–	–	0.02	2.6×10^{-3}	0.84	15	–	–	0.06	4.9×10^{-3}	0.94	7
12	–	–	0.03	2.1×10^{-3}	0.86	15	0.25	1.5×10^{-1}	0.02	4.8×10^{-3}	0.98	8
13	0.00	5.0×10^{-4}	0.01	1.9×10^{-3}	0.59	15	–	–	0.00	3.5×10^{-4}	0.75	8

Ranges of pigment concentration for which the parameters are given:

chl a: 0–0.5 mg m^{-3}; chl-c: 0–0.2 mg m^{-3};   chl a: 0–4.8 mg m^{-3}; chl c: 0–1.6 mg m^{-3};
chl b: 0–0.1 mg m^{-3}; carot.: 0–0.6 mg m^{-3} chl b: 0–0.1 mg m^{-3}; carot.: 0–4.4 mg m^{-3}

Table 4. Centers (nm) and halfwidths (nm) of the 13 Gaussian bands corresponding to all the data pooled together and to each of the individual groups

Gaussian band (i)	Associated pigment	Pooled Center	Halfwidth	Group A Center	Halfwidth	Group B Center	Halfwidth	Group C Center	Halfwidth	Group D Center	Halfwidth
1	chl a	383	53.3	382	53.8	383	52.8	383	53.7	383	52.9
2	chl a	413	22.8	413	23.5	413	21.9	414	24.0	412	22.8
3	chl a	435	32.2	434	32.4	435	31.3	436	34.2	434	32.4
4	chl c	461	33.5	461	31.9	461	33.1	459	38.7	459	34.8
5	chl b	466	41.1	465	41.3	466	40.7	467	41.1	466	42.8
6	carot.	490	49.7	491	48.2	489	50.4	488	51.3	490	49.6
7	carot.	530	52.3	531	52.7	530	51.6	530	53.8	530	52.1
8	chl c	584	53.4	584	53.3	584	53.0	582	55.4	586	52.1
9	chl a	622	37.9	622	36.4	622	39.4	620	38.1	623	35.5
10	chl c	645	31.1	645	34.1	645	29.8	643	27.9	644	30.0
11	chl b	658	28.3	658	30.6	657	26.8	657	24.9	658	31.8
12	chl a	674	25.9	674	27.5	675	24.3	674	26.1	674	27.6
13	chl a	699	38.3	699	38.5	699	38.3	699	37.9	700	36.1
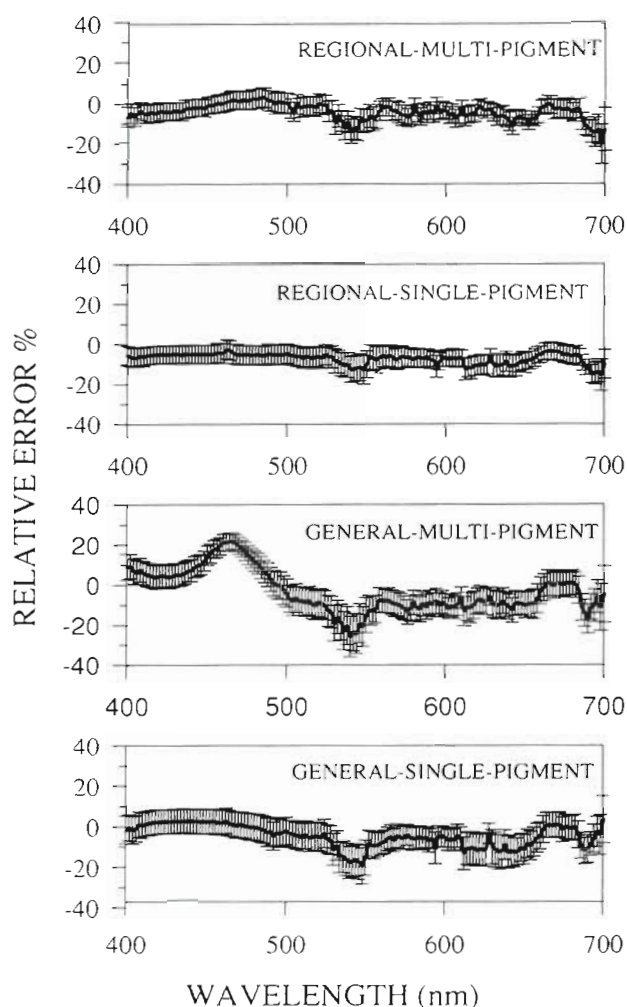
Fig. 10. Average, relative error (%) in the estimation of the shape of the absorption spectra of phytoplankton, for the 2 methods used in the 2 approaches. The bars show the standard errors of the average values

was also investigated at 6 selected wavelengths (i.e. SeaWiFS bands: 412, 443, 490, 510, 555, and 670 nm). Results are shown in Fig. 11 and Table 5.

DISCUSSION

Separation into regions with similar absorption characteristics

For the 4 groups (Fig. 1) the variability in the shape of the absorption spectra was most pronounced between 450 and 550 nm. This is the region where the accessory chlorophylls and carotenoids have their maximum absorptions. So the changes in the composition of accessory pigments should affect this region more than anywhere else. These differences were, however, quite small, compared with the differences in the specific absorption of phytoplankton, as will be seen later.

Even though the classification into groups was based purely on the shape of the absorption spectra, the corresponding HPLC data brought to light the underlying differences in species composition (Fig. 3).

Thus, Group A included samples from coastal areas which had low near-surface temperatures (~ 0 to 3°C). The main carotenoid in all samples from this group was fucoxanthin, which suggests that the phytoplankton communities were dominated by diatoms. However, fucoxanthin is also found in prymnesiophytes, chrysophytes and raphidophytes (Rowan 1989, Johnsen et al. 1994a), therefore the presence of any of these groups cannot be ruled out.

Group B corresponded to open-ocean samples which had high near-surface temperatures (~15 to 20°C, with the exception of stations in the Labrador
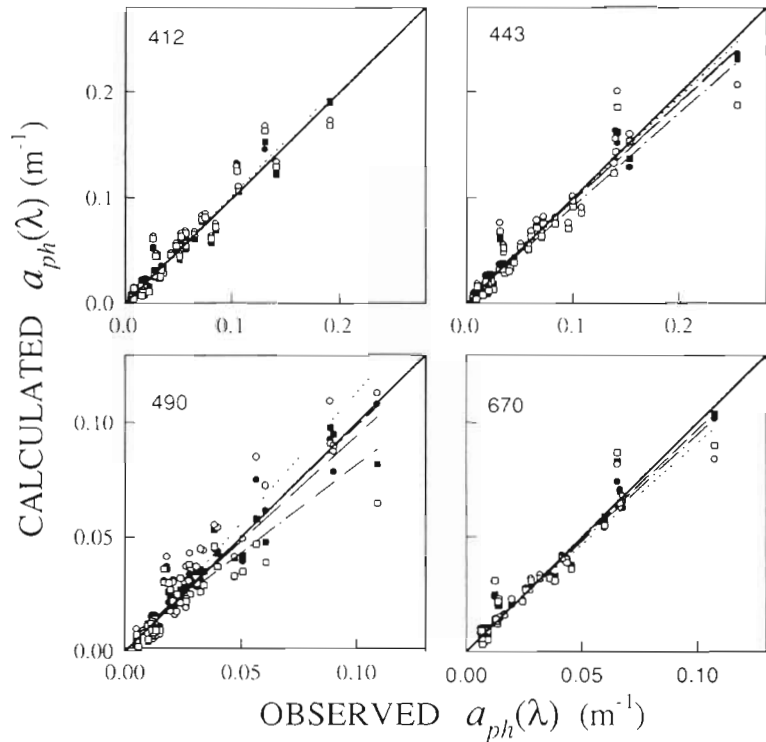
Fig. 11 Comparison, at a selected set of wavelengths, between observed and calculated phytoplankton absorption $[a_{ph}(\lambda)]$, using the 2 methods in the 2 approaches. 'General approach': hollow circles and dotted regression line for the 'single-pigment' method; and hollow squares and dot-dashed regression line for the 'multi-pigment' method. 'Regional approach': filled circles and small-dashed regression line for the 'single-pigment' method; filled squares and long-dashed regression line for the 'multi-pigment' method. The solid line represents the 1:1 slope

Sea and in the Greenland Current where temperatures were ~4°C) and lower concentrations of nitrate and chl a than areas corresponding to Group A. The main carotenoid in Group B was 19'-hexanoyloxyfucoxanthin, which indicated that prymnesiophytes were the predominant phytoplankton. Prymnesiophytes can be divided into 2 groups: those that possess chlorophyll c_3 and those that do not (e.g. *Isochrysis galbana*). This affects the absorption characteristics of the algae (Johnsen et al. 1994a), but a distinction as fine as this was not attempted in this study.

Group C also contained samples from oligotrophic waters, but these samples were characterized by high concentrations of zeaxanthin along with 19'-hexanoyloxyfucoxanthin. Zeaxanthin is found in prochloro-

phytes, cyanophytes and chlorophytes. Divinyl-chl a and divinyl-chl b, which are pigments specific to prochlorophytes (Chisholm et al. 1992), were also detected in these samples. Therefore, we can be sure that prochlorophytes were present in Group C, although cyanophytes and prymnesiophytes may have been present as well.

Group D represents a small number of samples from the open ocean located in, or close to, areas of higher nitrate concentrations (Stns 40, 78, 79). In this group fucoxanthin was the main carotenoid. Its location in the open ocean and the relatively low concentrations of silicates at these stations might indicate the presence of prymnesiophytes. The prymnesiophyte *Phaeocystis* sp., showing high concentrations of fucoxanthin,

Table 5. Correlations between observed and calculated absorption for the different methods tested, at the wavelengths to be monitored by the SeaWiFS satellite

λ (nm)	'Regional approach'						λ (nm)	'General approach'					
	'Multi-pigment'			'Single-pigment'				'Multi-pigment'			'Single-pigment'		
	Slope	SE	r^2	Slope	SE	r^2		Slope	SE	r^2	Slope	SE	r^2
412	0.997	0.040	0.94	0.994	0.039	0.94	412	1.001	0.047	0.92	1.032	0.049	0.92
443	0.943	0.033	0.96	0.934	0.034	0.95	443	0.894	0.047	0.90	0.971	0.051	0.90
490	0.922	0.048	0.91	0.967	0.046	0.92	490	0.768	0.060	0.81	1.146	0.060	0.91
510	0.891	0.053	0.89	0.981	0.054	0.91	515	0.832	0.075	0.79	1.107	0.067	0.89
555	0.903	0.090	0.83	0.958	0.109	0.79	555	0.917	0.118	0.75	0.939	0.095	0.83
670	0.998	0.035	0.96	0.955	0.030	0.97	670	0.931	0.049	0.91	0.886	0.047	0.91

was found near Stn 40 and off the coast of Newfoundland in spring (Head & Horne 1993, Head pers. comm.). The presence of high concentrations of phytoplankton at Stns 78 and 79 may be related to the Polar Front (Dietrich 1965, Lazier 1973), where spring blooms of *Phaeocystis* sp. have been reported by other authors (Wassman et al. 1990, Smith 1993, 1994). These previous, and later (WOCE cruise 1994 unpubl. data), studies in the area support the idea that the presence of *Phaeocystis* sp. is a characteristic feature of the spring bloom in the Polar Front region. Since no microscopic identifications were made however, the presence of diatoms or other prymnesiophytes having a high fucoxanthin to chl *a* ratio cannot be excluded. Therefore, we will refer to Group D as consisting of some prymnesiophytes or diatoms, while bearing in mind that these populations had several characteristics which distinguished them from both Group A (predominantly diatoms) and Group B (predominantly prymnesiophytes).

A similar study of phytoplankton absorption characteristics in the Gulf of Maine and Georges Bank (Hoepffner & Sathyendranath 1992) also showed clear regional differences in shape and amplitude of the specific absorption spectra. Studies on phytoplankton distribution and taxonomic composition have been carried out in the northeastern coastal waters of the United States over a period of 9 yr (reviews in Marshall & Cohn 1983, Matta & Marshall 1984). Some characteristics of the distribution of phytoplankton have emerged from these studies, such as the abundance of diatoms close to coastal areas and prymnesiophytes in the open ocean. Samples taken in 1992 from an autumn cruise in the North Atlantic along a transect passing near our Stn 3 and between our Stns 49 and 52 (Head unpubl. data) had pigment compositions similar to those reported here for the spring season. For example, samples taken close to Stn 3 (Group A) showed high concentrations of fucoxanthin; and samples taken close to Stns 49 and 52 (Group C) showed high concentrations of 19'-hexanoyloxyfucoxanthin and zeaxanthin, together with both divinyl-chl *a* and divinyl-chl *b*. On the other hand, in samples collected during spring of 1990 (Head & Horne 1993), close to Stn 49 (Group C), the main carotenoid was fucoxanthin, which was probably associated with the prymnesiophyte *Phaeocystis* sp.

The results of the studies carried out by Marshall & Cohn (1983) and Matta & Marshall (1984) have demonstrated that year-to-year variations can be important, but that if this long-term variation is removed, seasonal and geographical patterns of distribution can also be detected. Thus, year-to-year variations (Matta & Marshall 1984), as well as short-term variations, like those produced by the intrusion of water from other areas

(Head & Horne 1993), may affect the regional distribution of phytoplankton. The influence of these variations on the pattern of distribution of phytoplankton parameters will be better understood when more field data become available. On the whole, however, even if the regions of distinct absorption characteristics are subject to long-term and short-term variations, partitioning the ocean into regions where these parameters can be considered to be quasi-stable, taking into account the major trends in their distribution, will be an improvement on assuming general characteristics for the whole ocean.

Variability of the *in vivo* absorption coefficient [a^*_m or $p^*_m(i)$]

Factors influencing the absorption coefficient

In principle, absorption of light by phytoplankton pigments follows Beer's Law, i.e. absorption increases linearly with pigment concentration. However, when dealing with *in vivo* absorption by phytoplankton cells, this linear relationship is affected by 2 additional factors: pigment composition and the flattening effect (Sathyendranath et al. 1987). Since the total phytoplankton absorption at a given wavelength is the sum of the contributions from each of the pigments to absorption at that wavelength, changes in pigment composition will certainly affect the relationship between absorption and chl *a* concentration in the case of the 'single-pigment' method, and this effect cannot be completely ruled out in the case of the 'multi-pigment' method used here either. The flattening effect refers to the relative flattening of the absorption spectrum of particles in suspension relative to that of the same material in solution (Duysens 1956). It depends on the particle size and shape and on the concentration of the absorbing material within the cells. It is known that the specific absorption coefficients (absorption normalised to chl *a* concentration) decrease with cell-size and intracellular pigment concentrations (Morel & Bricaud 1981). In fact, in the natural environment low chlorophyll concentrations are often associated with a predominance of small phytoplankton cells, and high chlorophyll concentrations with large cells (Yentsch & Phinney 1989). As a consequence, the relationship between absorption and pigments is often non-linear (Prieur & Sathyendranath 1981, Morel 1991, Cleveland 1995). Changes in cell-size will cause deviations from linearity in the relationship between absorption and pigment concentration regardless of whether the 'single-pigment' or the 'multi-pigment' method is used.

Probable cell-size distribution in this study

As mentioned, the flattening effect is affected by cell-size (Morel & Bricaud 1981, Sathyendranath et al. 1987, Cleveland 1995). Although cell-sizes were not measured in our study, a plausible ranking of cell-size among groups can be made based on the information about algal composition provided by the HPLC analysis (i.e. the most probable but not definitive algal composition) Group A (predominantly diatoms) should have the largest cells; then in decreasing order of cell-size would be Groups D (prymnesiophytes and/or diatoms) and B (predominantly prymnesiophytes); and finally, Group C (a mixture of prymnesiophytes, prochlorophytes and cyanophytes).

Variations in the absorption parameters in this study

In the rectangular hyperbola function used here, the parameter $a^{\bullet}_m$ [or $p^{\bullet}_m(i)$] is the initial slope of the curve depicting absorption as a function of pigment concentration, and represents the maximum specific absorption coefficient for that group of data. In principle, this maximum should approach the value of specific absorption in the absence of flattening effect, if indeed flattening effect decreases with ambient pigment concentrations.

For the case of the 'single-pigment' method ('regional approach'), an inverse relationship was found between the presumed cell-size distribution and the values of $a^{\bullet}_m$ (Group C < Group B < Group D < Group A; Table 1), probably indicating residual influence of flattening effect. In the 'multi-pigment' method ('regional approach'), the values of $p^{\bullet}_m(i)$ corresponding to the 2 absorption maxima of chl a in vivo (Gaussian bands $i = 3$ and $i = 12$) also show an inverse relationship with the expected size distribution, with the values of $p^{\bullet}_m(3)$ and $p^{\bullet}_m(12)$ for Groups A and D being significantly lower than those of Groups B and C (Table 3).

The values of $p^{\bullet}_m(12)$, representing absorption by chl a at 674 nm, [ranging from 0.021 m^{-1} (mg chl a m^{-3})$^{-1}$ for Group A to 0.037 m^{-1} (mg chl a m^{-3})$^{-1}$ for Group B] are higher than those previously reported for the in vivo specific coefficient of chl a at that wavelength [~0.020 m^{-1} (mg chl a m^{-3})$^{-1}$; Bricaud et al. 1983, Bidigare et al. 1987, 1990, Hoepffner & Sathyendranath 1991, 1993]. These higher values of $p^{\bullet}_m(12)$ might arise from various causes: (1) the estimation of $p_m(i)$ depends on the low values of absorption, and in some cases, especially for Groups B and C, these values were close to the limit of detection of the spectrophotometer, which would increase the error in the estimates; (2) the absorption

by pigments other than chl a may not have been completely corrected for by the method used here, although that possibility is minimum at 674 nm; and (3) finally, we should not underestimate the possibility that the high values of $p^{\bullet}_m(i)$ represent real variability in the specific absorption coefficient of chl a in vivo compared with that in vitro. Johnsen et al. (1994b), using chromoproteins isolated from dinoflagellates, estimated an in vivo specific absorption coefficient of chl a at 675 nm of 0.027 m^{-1} (mg chl a m^{-3})$^{-1}$, and suggested that this value could vary with species and with the photoadaptational changes in pigment composition.

With respect to the other major pigments, the values of $p^{\bullet}_m(i)$ for chl c ($i = 4$, 8 and 10) follow the same tendency as those of chl a, with the $p^{\bullet}_m(i)$ values for Groups A and D being significantly lower than those of Groups B and C. On the other hand, this tendency is not seen in the $p^{\bullet}_m(i)$ values for chl b or carotenoids (Table 3). Chl b concentrations were generally low, and the fits were consequently poor for this pigment (Figs. 8 & 9, Table 3) and therefore these values should be treated with caution. In the case of carotenoids (Table 3, $i = 6$ and 7), the variability in the values of $p^{\bullet}_m(i)$ might be due to the fact that all the carotenoids are summed together, so that these differences could reflect changes in the composition of carotenoids. Furthermore, carotenoids from different cell types are packaged differently within protein complexes and chloroplasts. Finally, we cannot discount the possibility of influence of phycobilins (~ 480 to 600 nm) which were not measured in these samples.

Comparison between different methods of estimating the absorption coefficient of phytoplankton

The use of the 'regional approach' resulted in low relative errors (~10%) in the reconstruction of the absorption spectrum by both the 'multi-pigment' and the 'single-pigment' methods (Fig 10). The distribution of relative errors was almost spectrally neutral, implying that the shape of the spectra was preserved in the reconstruction. The performance of the 'single-pigment' method is comparable to that of the 'multi-pigment' method in the 'regional approach' and has the virtue of simplicity: the absorption coefficient of phytoplankton can be predicted knowing the relevant parameters for each region and the chl a concentration alone, which can be estimated over large spatial scales by remote sensing. Inversely, prior knowledge of regional variations in the absorption characteristics could be used to improve regional algorithms for pigment retrieval. On the other hand, the 'multi-pigment'

method has the potential for accounting for the influence of specific pigments.

The performance of the 'general approach', using both the methods ('single-' and 'multi-pigment'), is slightly lower than that of the 'regional approach' (Fig 10). In the case of the 'single-pigment' method the errors are low except in the region of minimum absorption (~20% at ~550 nm) The high errors (~20%) associated with the 'multi-pigment' method in the blue-green region of the spectrum can be explained mainly by the differences observed in the specific peak heights of chl b between groups (Table 3), and consequent deterioration in fitting when all the data are pooled together (Fig. 8).

The comparison between observed and calculated absorption coefficients at the 6 SeaWiFS wavelengths is good in general for all the methods (Fig 11, Table 5). However, as noticed in the spectral distribution of errors in the blue-green part of the spectrum (490, 510 nm), the 'regional approach' (using both the 'multi-' and 'single-pigment' methods) performed better (i.e. slopes closer to 1; Table 5) than the 'general approach'. The maximum deviations from the 1:1 slope were found with the 'general approach' implemented by the 'multi-pigment' method. These probably reflect the influence of the differences in specific peak heights for chl b among the different groups. In the case of the 'single-pigment' method the deviations from the 1:1 slope (Table 5) may simply reflect the higher variability in the shape of the average absorption spectrum at those wavelengths (Fig. 1).

Shape of the absorption spectra and specific absorption at 440 nm

Except for the blue-green region of the spectrum, there are no major differences in the shape of the normalised absorption spectrum among the groups (Fig. 1). On the other hand, the average normalised spectrum from all the samples combined shows significant differences in shape when compared with other average phytoplankton spectra from previous studies (Prieur & Sathyendranath 1981, Hoepffner & Sathyendranath 1993) (Fig. 12). There is also a significant difference between the relationship of absorption at 440 nm and chl a concentration in our data ($a^*_m = 0.07$ and $\bar{a}_m = 0.48$) compared with that given by Sathyendranath & Platt (1988) ($a^*_m = 0.06$ and $a_m = 0.35$). This may be due in part to differences in pigment composition among the samples used to derive those specific absorption coefficients, since the total absorption at 440 nm is influenced by absorption of most of the accessory pigments. In addition, differences in the data base and in the techniques of data collection may also influence the results. Prieur &
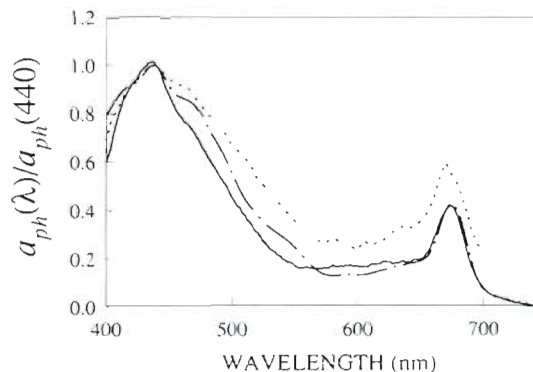

Fig. 12. Average, normalised absorption spectra of phytoplankton [$a_{ph}(\lambda)$]: average of the whole data set used in this study, solid line; average spectrum given by Prieur & Sathyendranath (1981), dotted line; average spectrum given by Hoepffner & Sathyendranath (1993), dot-dashed line

Sathyendranath (1981) derived their absorption from *in situ* irradiance measurements, whereas our results and those of Hoepffner & Sathyendranath (1993) are based on the filter technique.

CONCLUSIONS

The absorption characteristics of phytoplankton in the northwestern Atlantic in early spring show a geographical pattern of distribution. Thus, using a 'regional approach' in either the 'multi-pigment' or the simple 'single-pigment' method gives a better representation (within 10% relative error) of the absorption coefficient of phytoplankton than the 'general approach'. The improved performance of the regional method reflects regional changes in species composition or physiological state of phytoplankton populations. The differences in the shapes of the absorption spectra between regions are small. On the other hand, the parameters which determine the magnitude of absorption for a given pigment concentration were more variable. Note, however, that the 'single-pigment' method in the context of the 'general approach' would still give acceptable results (within 20% relative error in the region of low absorption in the green, and lower errors elsewhere) for many applications.

This approach is a compromise between global studies (Garver et al. 1994) and specific studies on unialgal cultures or on photoadaptation in a particular location (Kiefer et al. 1979, SooHoo et al. 1986, Sathyendranath et al. 1987, Takahashi et al. 1989, Bidigare et al. 1990, Sosik & Mitchell 1991, Johnsen et al. 1994a, b). On the whole, regional differences in optical characteristics of phytoplankton, though small, contain useful information, and could be used to improve remote-sensing algorithms.

Appendix 1. Symbols used in this paper, and their description and units

$a_d(440)$	Absorption by detritus at 440 nm, m^{-1}
a_∞	Maximum value of absorption at the plateau of the absorption vs pigment concentration curve, m^{-1}
a^*_{∞}	Maximum specific absorption coefficient, m^{-1} (mg chl a m^{-3})$^{-1}$
$a_p(\lambda)$	Absorption coefficient of particles in suspension at wavelength λ, m^{-1}
$a_{pf}(\lambda)$	Absorption coefficient of particles on the filter at wavelength λ, m^{-1}
$a_{ph}(\lambda)$	Absorption coefficient of phytoplankton at wavelength λ, m^{-1}
a^*_{ph}	Specific absorption coefficient of phytoplankton, m^{-1} (mg chl a m^{-3})$^{-1}$
$a'_{ph}(\lambda)$	Absorption coefficient of phytoplankton at wavelength λ normalised to 440 nm, dimensionless
C_i	Pigment concentration, mg pigment i m^{-3}
D	Optical density or absorbance, dimensionless
$K_d(\lambda)$	Diffuse attenuation coefficient of downwelling light, m^{-1}, at wavelength λ
$p_i(\lambda_i)$	Peak height at the wavelength of the center of the ith Gaussian band, m^{-1}
$p_m(i)$	Maximum value of absorption at the plateau of the peak height vs pigment concentration curve, corresponding to the ith Gaussian band, m^{-1}
$p^*_m(i)$	Maximum specific peak height corresponding to the ith Gaussian band, m^{-1} (mg pigment i m^{-3})$^{-1}$
P^B_m	Maximum production at high light normalised to biomass, mg C (mg chl a)$^{-1}$ h^{-1}
q	Exponent in the function describing the spectral form of detrital absorption (see Eq. 3)
X	Height of the water column filtered (m), given by V/S, where V = volume of seawater filtered (m^3) and S = filtering area of the filter (m^2)
W_i	Halfwidth of the ith Gaussian band, nm
α^B	Photosynthetic efficiency at low light normalised to biomass, mg C (mg chl a)$^{-1}$ h^{-1} (W m^{-2})$^{-1}$
β	Pathlength amplification factor, dimensionless
λ	Wavelength
λ_i	Wavelength of the center of the ith Gaussian band, nm

LITERATURE CITED

Bidigare RR, Morrow JH, Kiefer DA (1989) Derivative analysis of spectral absorption by photosynthetic pigments in the western Sargasso Sea. J Mar Res 47:323–341

Bidigare RR, Ondrusek ME, Morrow JH, Kiefer DA (1990) *In vivo* absorption properties of algal pigments. SPIE Proceedings, Ocean Optics X 1302:290–302

Bidigare RR, Smith RC, Baker KS, Marra J (1987) Oceanic primary production estimates from measurements of spectral irradiance and pigment concentrations. Global Biogeochem Cycles 1:171–186

Bricaud A, Morel A, Prieur L (1983) Optical efficiency factors of some phytoplankters. Limnol Oceanogr 28:816–832

Bricaud A, Stramski D (1990) Spectral absorption coefficients of living phytoplankton and nonalgal biogenous matter: a comparison between the Peru upwelling area and the Sargasso Sea. Limnol Oceanogr 35:562–582

Butler WL (1962) Absorption of light by turbid materials. J Opt Soc Am 52:292–299

Chisholm SW, Frankel SL, Goericke R, Olson RJ, Palenik B, Waterbury JB, West-Johnsrud L, Zettler ER (1992) *Prochlorococcus marinus* nov. gen. sp.: an oxyphototrophic marine prokaryote containing divinyl chlorophyll *a* and *b*. Arch Microbiol 157:297–300

Cleveland JS (1995) Regional models for phytoplankton absorption of chlorophyll *a* concentration. J Geophys Res 100:13333–13344

Cleveland JS, Weidemann AD (1993) Quantifying absorption by aquatic particles: a multiple scattering correction for glass-fiber filters. Limnol Oceanogr 38:1321–1327

Dietrich G (1965) New hydrographical aspects of the Northwest Atlantic. Int Commission for the Northwest Atlantic Fisheries, ICNAF Spec Publ 6:29–51

Duysens LNM (1956) The flattening of the absorption spectrum of suspensions, as compared to that of solutions. Biochim Biophys Acta 19:1–12

Eppley RW, Stewart E, Abbott MR, Heyman U (1985) Estimating ocean primary production from satellite chlorophyll. Introduction to regional differences and statistics for the Southern California Bight. J Plankton Res 7:57–70

Everitt DA, Wright SW, Volkman JK, Thomas DP, Lindstrom EJ (1990) Phytoplankton community compositions in the western equatorial Pacific determined from chlorophyll and carotenoid pigment distributions. Deep Sea Res 37:975–997

Garver SA, Siegel D, Mitchell BG (1994) Variability in near-surface particulate absorption spectra: What can a satellite ocean color imager see? Limnol Oceanogr 39:1349–1367

Gieskes WWC, Kraay GW, Nontji A, Setiapermana D, Sutomo (1988) Monsoonal alternation of a mixed and a layered structure in the phytoplankton of the euphotic zone of the Banda Sea (Indonesia): a mathematical analysis of algal pigment fingerprints. Neth J Sea Res 22:123–127

Gordon HR, Morel A (1983) Remote assessment of ocean colour for interpretation of satellite visible imagery. A review. Lecture notes on coastal and estuarine studies, Vol 4, Springer-Verlag, New York

Head EJH, Horne EPW (1993) Pigment transformation and vertical flux in an area of convergence in the North Atlantic. Deep Sea Res 40:329–346

Hoepffner N, Sathyendranath S (1991) Effect of pigment composition on absorption properties of phytoplankton. Mar Ecol Prog Ser 73:11–23

Hoepffner N, Sathyendranath S (1992) Bio-optical characteristics of coastal waters: absorption spectra of phytoplankton and pigment distribution in the western North Atlantic. Limnol Oceanogr 8:1660–1679

Hoepffner N, Sathyendranath S (1993) Determination of the major groups of phytoplankton pigments from the absorption spectra of total particulate matter. J Geophys Res 98:22789–22803

Hooker SB, Esaias WE, Feldman GC, Gregg WW, McClain CR (1992) An overview of SeaWiFS and ocean color. In: Hooker SB, Firestone ER (eds) SeaWiFS Technical Report Series. NASA Tech Mem 104566, Vol 1, NASA, Greenbelt, MD

Johnsen G, Nelson NB, Jovine RVM, Prezelin BB (1994b) Chromoprotein- and pigment-dependent modeling of spectral light absorption in two dinoflagellates, *Prorocentrum minimum* and *Heterocapsa pygmaea*. Mar Ecol Prog Ser 114:245–258

Johnsen G, Samset O, Granskog L, Sakshaug E (1994a) In vivo absorption characteristics in 10 classes of bloom-forming phytoplankton: taxonomic characteristics and responses to photoadaptation by means of discriminant and HPLC analysis. Mar Ecol Prog Ser 105:149–157

Kiefer DA, Mitchell BG (1983) A simple steady state description of phytoplankton growth based on absorption cross section and quantum efficiency. Limnol Oceanogr 28:770–776

Kiefer DA, Olson RJ, Wilson WH (1979) Reflectance spectroscopy of marine phytoplankton. Part 1 Optical properties as related to age and growth rate. Limnol Oceanogr 24:664–672

Kiefer DA, SooHoo JB (1982) Spectral absorption by marine particles of coastal waters of Baja California. Limnol Oceanogr 27:492–499

Kirk JTO (1983) Light and photosynthesis in aquatic ecosystems. Cambridge University Press, Cambridge

Kishino M, Takahashi M, Okami N, Ichimura S (1985) Estimation of the spectral absorption coefficients of phytoplankton in the sea. Bull Mar Sci 37:634–642

Lazier JRN (1973) The renewal of Labrador Sea Water. Deep Sea Res 20:341–353

Lewis MR (1987) Phytoplankton and thermal structure in the Tropical Ocean. Oceanol Acta Proceedings International Symposium on Equatorial Vertical Motion, Paris, 6–10 May 1985. Gauthier-Villars, Montrouge, p 91–95

Lewis MR, Cullen JJ, Platt T (1983) Phytoplankton and thermal structure in the upper ocean: consequence of nonuniformity in chlorophyll profile. J Geophys Res 88:2565–2570

Lutz VA (1994) Variability of the specific absorption coefficient of phytoplankton in the Northwestern Atlantic. MSc thesis, Dalhousie University, Halifax

Marshall HG, Cohn MS (1983) Distribution and composition of phytoplankton in northeastern coastal waters of the United States. Estuar Coast Shelf Sci 17:119–131

Matta JF, Marshall HG (1984) A multivariate analysis of phytoplankton assemblages in the western North Atlantic. J Plankton Res 6:663–675

Mitchell BG, Kiefer DA (1984) Determination of absorption and fluorescence excitation spectra for phytoplankton. In: Holm-Hansen O, Bolis L, Gilles R (eds) Marine phytoplankton and productivity. Springer-Verlag, Berlin, p 157–169

Morel A (1978) Available, usable, and stored radiant energy in relation to marine photosynthesis. Deep Sea Res 25:673–688

Morel A (1988) Optical modeling of the upper ocean in relation to its biogenous matter content (Case I waters). J Geophys Res 93:749–10, 768

Morel A (1991) Light and marine photosynthesis: a spectral model with geochemical and climatological implications. Prog Oceanogr 26:263

Morel A, Bricaud A (1981) Theoretical results concerning light absorption in a discrete medium, and application to specific absorption of phytoplankton. Deep Sea Res 28:1375–1393

Platt T (1986) Primary production of the ocean water column as a function of surface light intensity: algorithms for remote sensing. Deep Sea Res 33:149–163

Platt T, Herman AW (1983) Remote sensing of phytoplankton in the sea: surface layer chlorophyll as an estimate of water-column chlorophyll and primary production. Int J Rem Sens 4:343–351

Platt T, Lewis M, Geider R (1984) Thermodynamics of the pelagic ecosystem: elementary closure conditions for biological production in the open ocean. In: Fasham MJR (ed) Flows of energy and materials in marine ecosystems. Plenum Publishing Corporation, New York, p 49–84

Platt T, Sathyendranath S (1988) Oceanic primary production: estimation by remote sensing at local and regional scales. Science 241:1613–1620

Platt T, Sathyendranath S, Caverhill CM, Lewis MR (1988) Ocean primary production and available light: further algorithms for remote sensing. Deep Sea Res 35:855–879

Platt T, Sathyendranath S, Ravindran P (1990) Primary production by phytoplankton: analytic solutions for daily rates per unit area of water surface. Proc R Soc Lond B 241:101–111

Platt T, Sathyendranath S, Ulloa O, Harrison WG, Hoepffner N, Goes J (1992) Nutrient control of phytoplankton photosynthesis in the Western North Atlantic. Nature 356:229–231

Platt T, Sathyendranath S, White GN, Ravindran P (1994) Attenuation of visible light by phytoplankton in a vertically structured ocean: solutions and applications. J Plankton Res 16:1461–1487

Prieur L, Sathyendranath S (1981) An optical classification of coastal and oceanic waters based on the specific spectral absorption curves of phytoplankton pigments, dissolved organic matter, and other particulate materials. Limnol Oceanogr 26:671–689

Roesler CS, Perry MJ, Carder KL (1989) Modeling in situ phytoplankton absorption from total absorption spectra in productive inland marine waters. Limnol Oceanogr 34:1510–1523

Rowan KS (1989) Photosynthetic pigments of algae. Cambridge University Press, Cambridge

Sathyendranath S, Gouveia AD, Shetye SR, Ravindran P, Platt T (1991) Biological control of surface temperature in the Arabian Sea. Nature 349:54–56

Sathyendranath S, Lazzara L, Prieur L (1987) Variations in the spectral values of specific absorption of phytoplankton. Limnol Oceanogr 32:403–415

Sathyendranath S, Morel A (1983) Light emerging from the sea — interpretation and uses in remote sensing. In: Cracknell AP (ed) Remote sensing applications in marine science and technology. D Reidel Publishing Company, Dordrecht, p 323–357

Sathyendranath S, Platt T (1988) The spectral irradiance field at the surface and in the interior of the ocean: a model for applications in oceanography and remote sensing. J Geophys Res 93:9270–9280

Sathyendranath S, Platt T (1989a) Remote sensing of ocean chlorophyll: consequence of non-uniform pigment profile. Appl Optics 28:490–495

Sathyendranath S, Platt T (1989b) Computation of aquatic primary production: extended formalism to include effect of angular and spectral distribution of light. Limnol Oceanogr 34:188–198

Smith RC, Baker KS (1978) Optical classification of natural waters. Limnol Oceanogr 23:260–267

Smith RC, Eppley RW, Baker KS (1982) Correlation of primary production as measured aboard ship in southern Califor-

nia coastal waters and as estimated from satellite chlorophyll images. Mar Biol 66:281–288

Smith RC, Marra J, Perry MJ, Baker KS, Swift E, Buskey E, Kiefer DA (1989) Estimation of a photon budget for the upper ocean in the Sargasso Sea. Limnol Oceanogr 34: 1673–1693

Smith WO (1993) Nitrogen uptake and new production in the Greenland Sea: the spring *Phaeocystis* bloom. J Geophys Res 98:4681–4688

Smith WO (1994) Primary productivity of a *Phaeocystis* bloom in the Greenland sea during spring 1989. In: The Polar Oceans and their role in shaping the global environment. Geophysical Monograph 85, American Geophysical Union, Washington, DC, p 263–272

SooHoo JB, Kiefer DA, Collins DJ, McDermid IS (1986) *In vivo* fluorescence excitation and absorption spectra of marine phytoplankton. I. Taxonomic characteristics and responses to photoadaptation. J Plankton Res 8:197–214

Sosik HM, Mitchell BG (1991) Absorption, fluorescence and quantum yield for growth in nitrogen-limited *Dunaliella tertiolecta*. Limnol Oceanogr 36:910–921

Stramski D (1990) Artifacts in measuring absorption spectra of phytoplankton collected on a filter. Limnol Oceanogr 35: 1804–1809

Takahashi M, Ichimura I, Kishino M, Okami N (1989) Shade and chromatic adaptation of phytoplankton photosynthesis in a thermally stratified sea. Mar Biol 100:401–409

Wassmann P, Vernet M, Mitchell BG, Rey F (1990) Mass sedimentation of *Phaeocystis pouchetii* in the Barents Sea. Mar Ecol Prog Ser 66:183–195

Wright SW, Jeffrey SW, Mantoura RFC, Llewellyn CA, Bjørnland T, Repeta D, Welshmeyer N (1991) Improved HPLC method for the analysis of chlorophylls and carotenoids from marine phytoplankton. Mar Ecol Prog Ser 77:183–196

Yentsch CS (1962) Measurement of visible light absorption by particulate matter in the ocean. Limnol Oceanogr 7:207–217

Yentsch CS, Phinney DA (1989) A bridge between ocean optics and microbial ecology. Limnol Oceanogr 34:1694–1705